

Vidyo meeting,
16.1.2014

Tests of the irradiated ATLAS-12 sensors

A.Chilingarov and H.Fox
Lancaster University, UK

Contents

1. Introduction
2. IV characteristics
3. CV and depletion voltage
4. Interstrip capacitance
5. Interstrip resistance
6. Punch-through properties
7. Conclusions

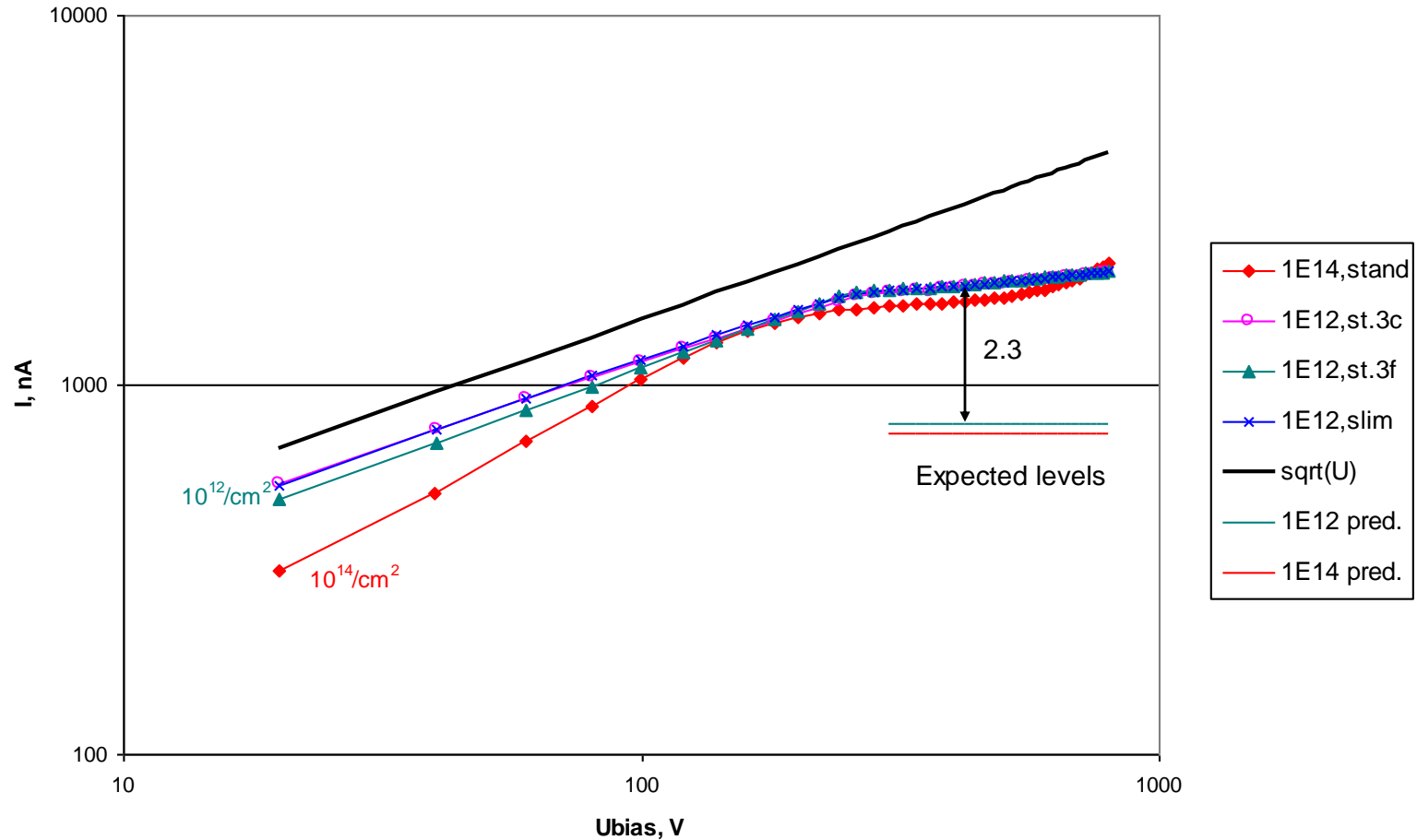
1. Introduction. Sensors and their irradiations

Sensor	Edge type	Fluence, neq/cm ²	Dose, Mrad
W631-BZ3C-P4	Standard	1E+12	0.115
W623-BZ3F-P3	Standard	1E+12	0.115
W607-BZ3C-P2	Slim	1E+12	0.115
W627-BZ3C-P12	Standard	1E+14	11.5
W610-BZ3C-P4	Slim	1E+14	11.5
W633-BZ3C-P12	Standard	1E+15	115
W627-BZ3F-P5	Standard	1E+15	115
W636-BZ3C-P12	Standard	5E+15	575

All sensors were irradiated by 27 MeV protons and annealed for 10 days at a temperature of $\sim 21^{\circ}\text{C}$. The sensors irradiated by 10^{12} neq/cm² were tested at the Probe Station at $+21^{\circ}\text{C}$. The other sensors were tested in a special DUT box typically at -25°C and sometimes at -35°C .

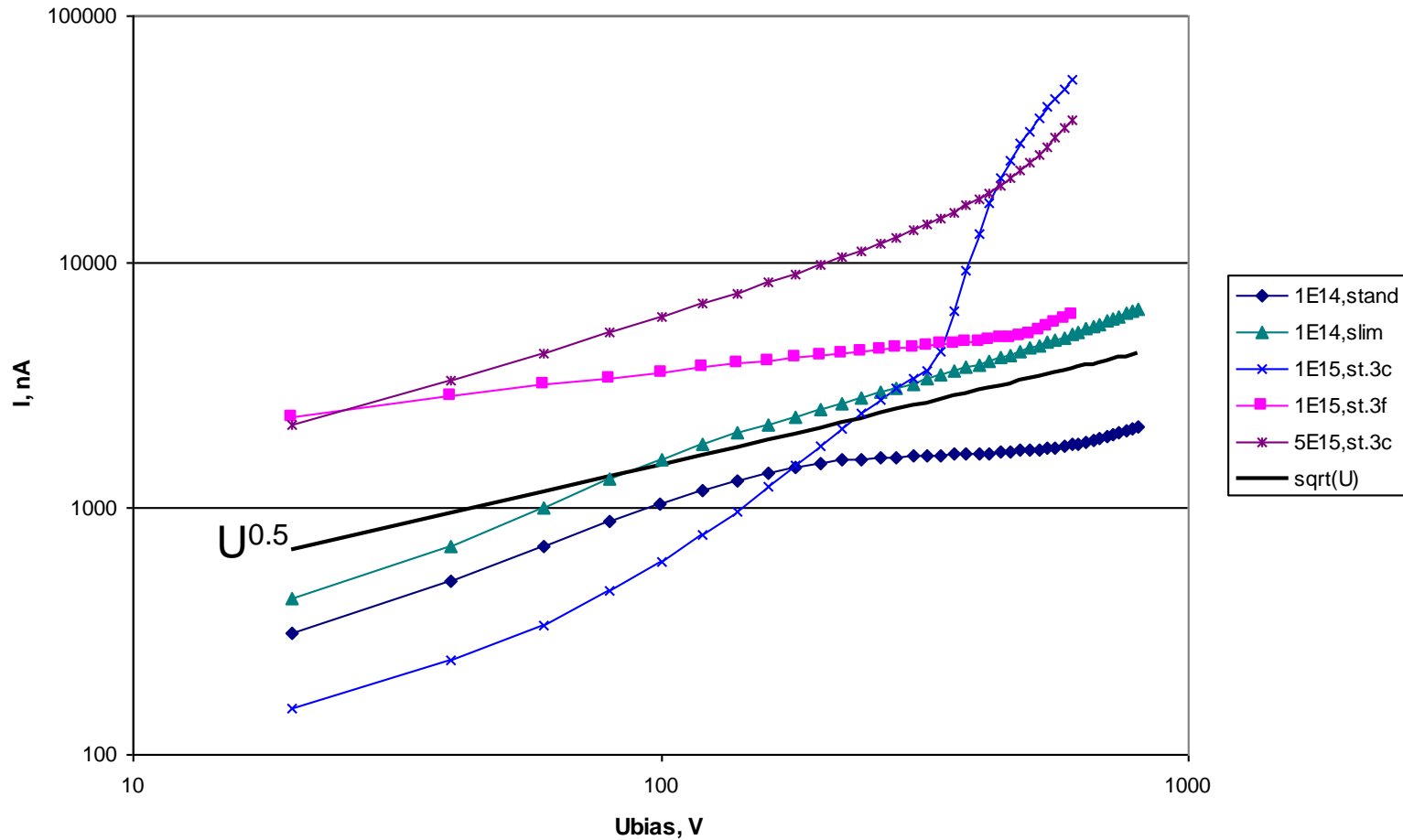
2. IV characteristics

Sensors irradiated by 10^{12} and 10^{14} neq/cm²: IV at +20C and -25C respectively



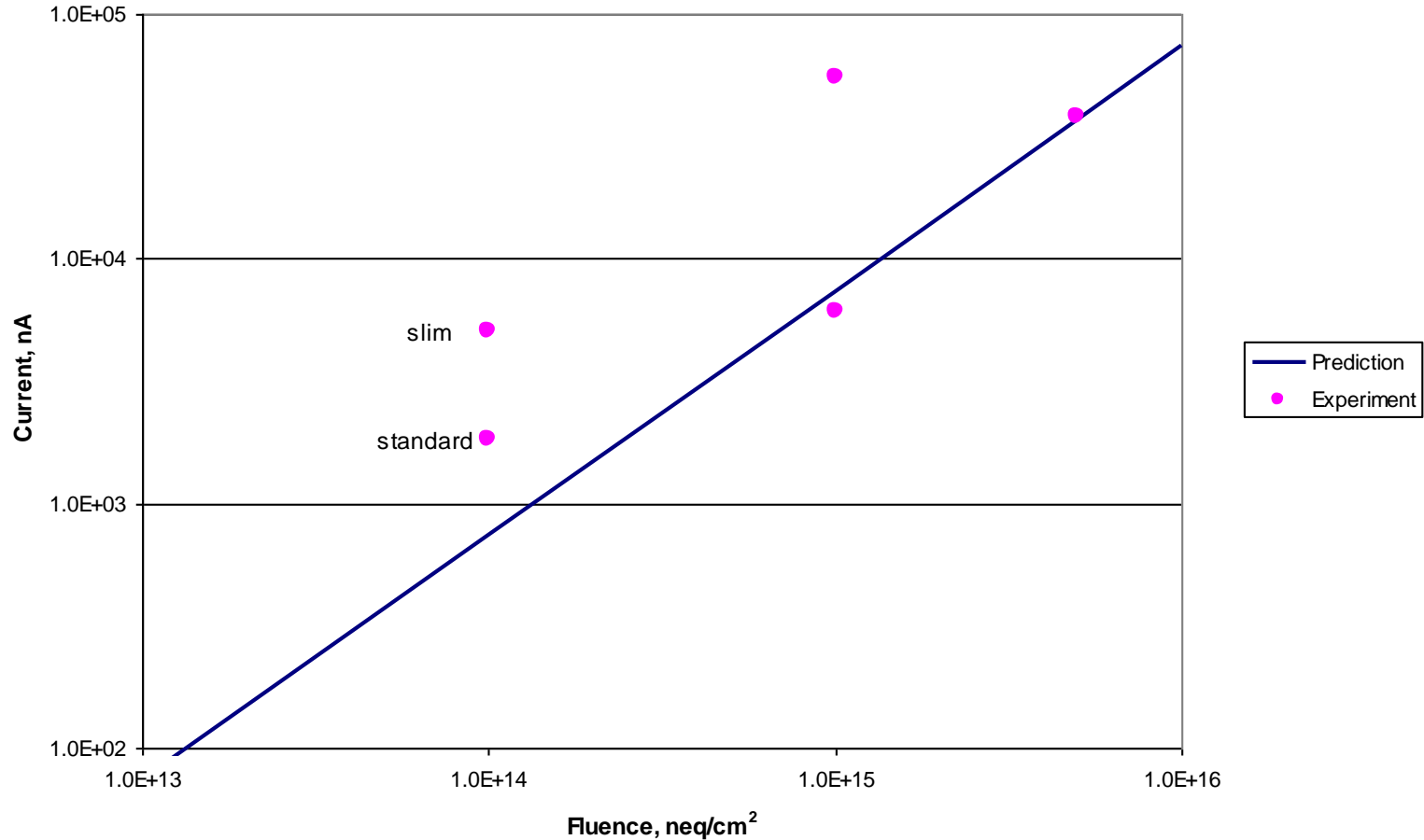
The IV curves for low fluence sensors. The black line shows $U^{0.5}$ dependence and the colour lines the levels expected from $\alpha(20^\circ\text{C})=4 \cdot 10^{-17}$ A/cm. Temperature correction coefficient between 20°C and -25°C was taken as 107.

IV at -25C for the sensors irradiated up to $5E15$ neq/cm²:



IV at -25°C for fluences 10^{14} – $5 \cdot 10^{15}$ neq/cm². Only the standard sensor irradiated by 10^{14} neq/cm² exhibits a kink allowing depletion voltage estimate.

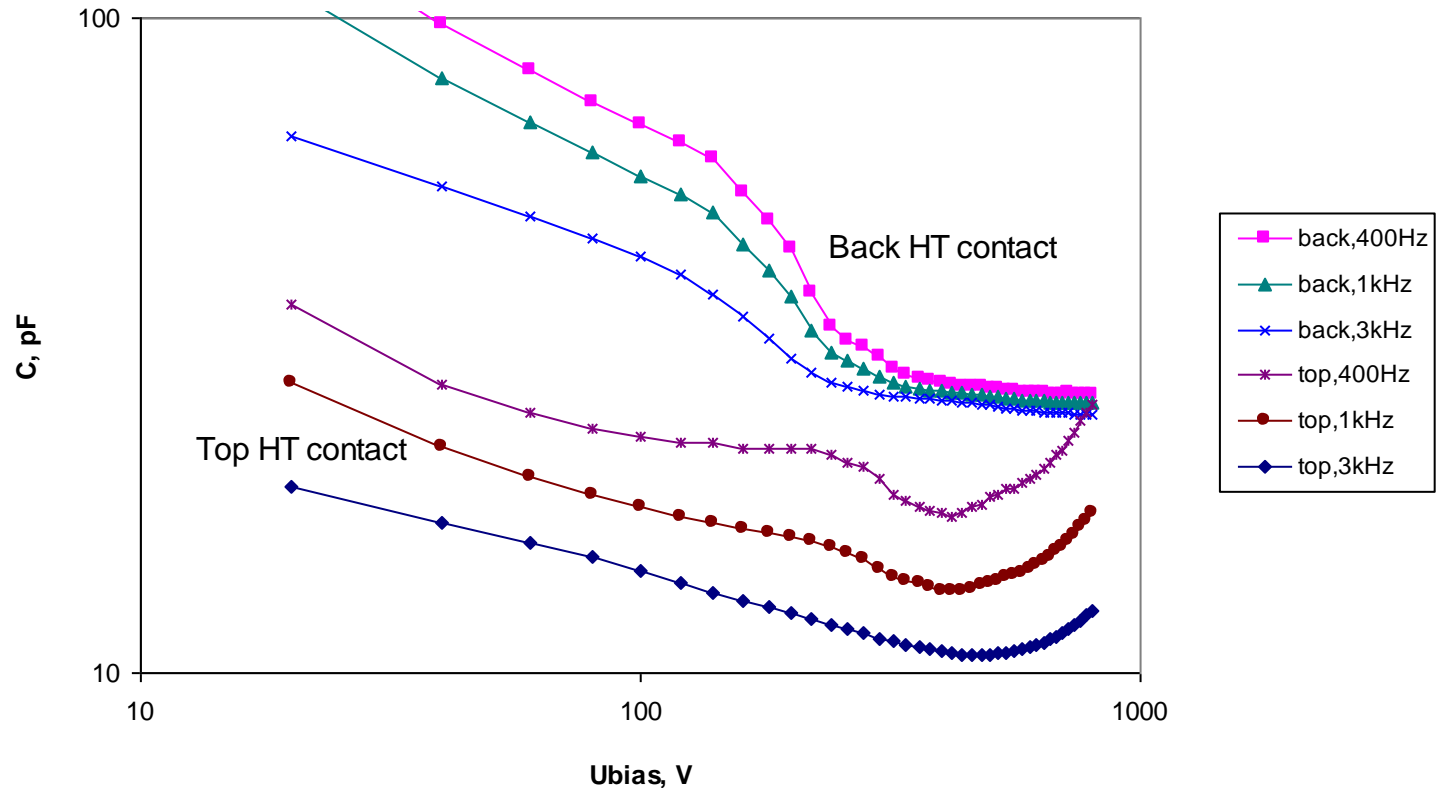
Predicted current at full depletion and measured at 600V for -25C



The current measured at 600V and expected for a fully depleted sensor. Note that for the fluence above 10^{14} neq/cm² the sensors are not depleted at 600V.

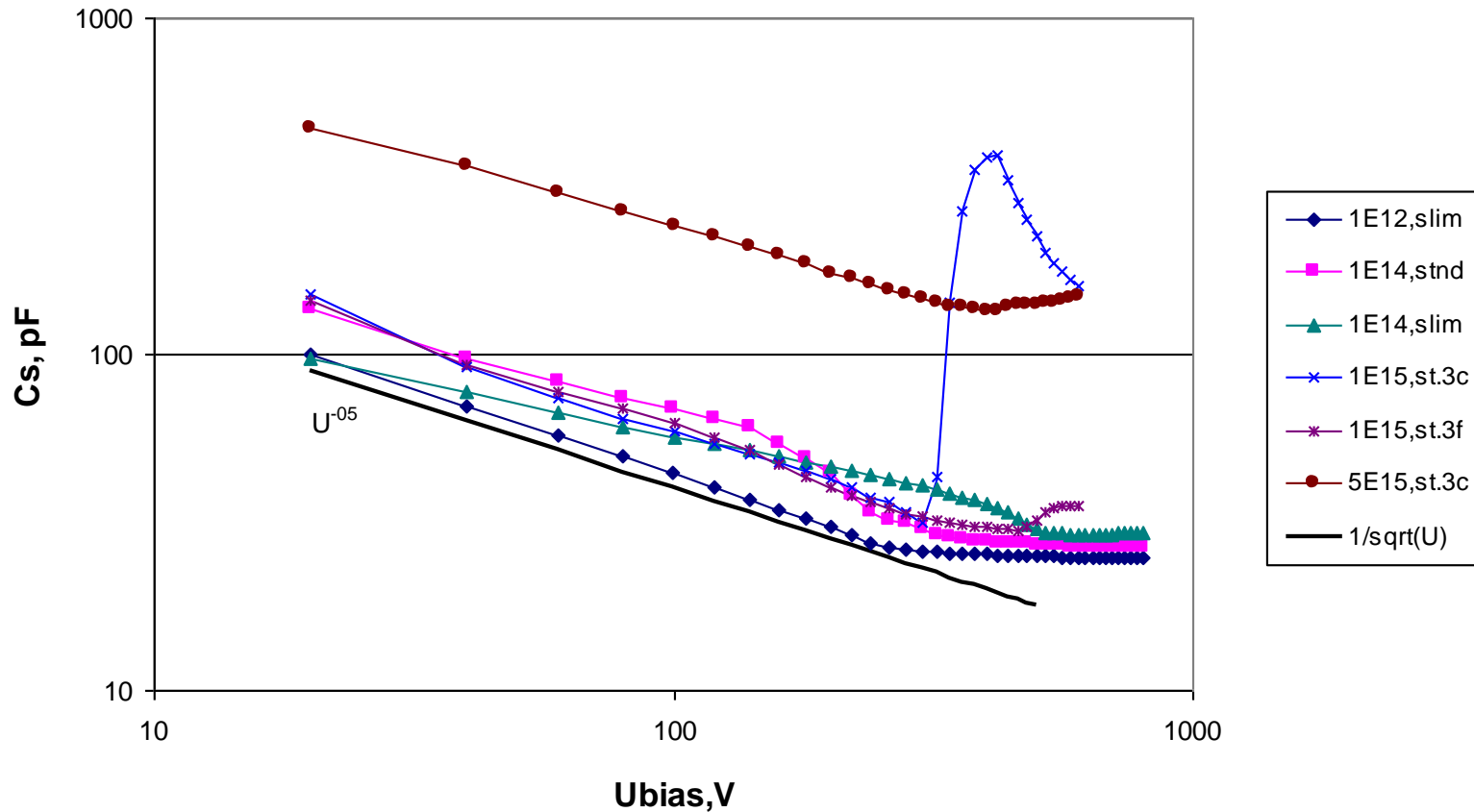
2. CV and depletion voltage

Standard w627-bz3c-p12 irradiated by $1E14$ neq/cm²: CV at -25C for back and top HT contacts



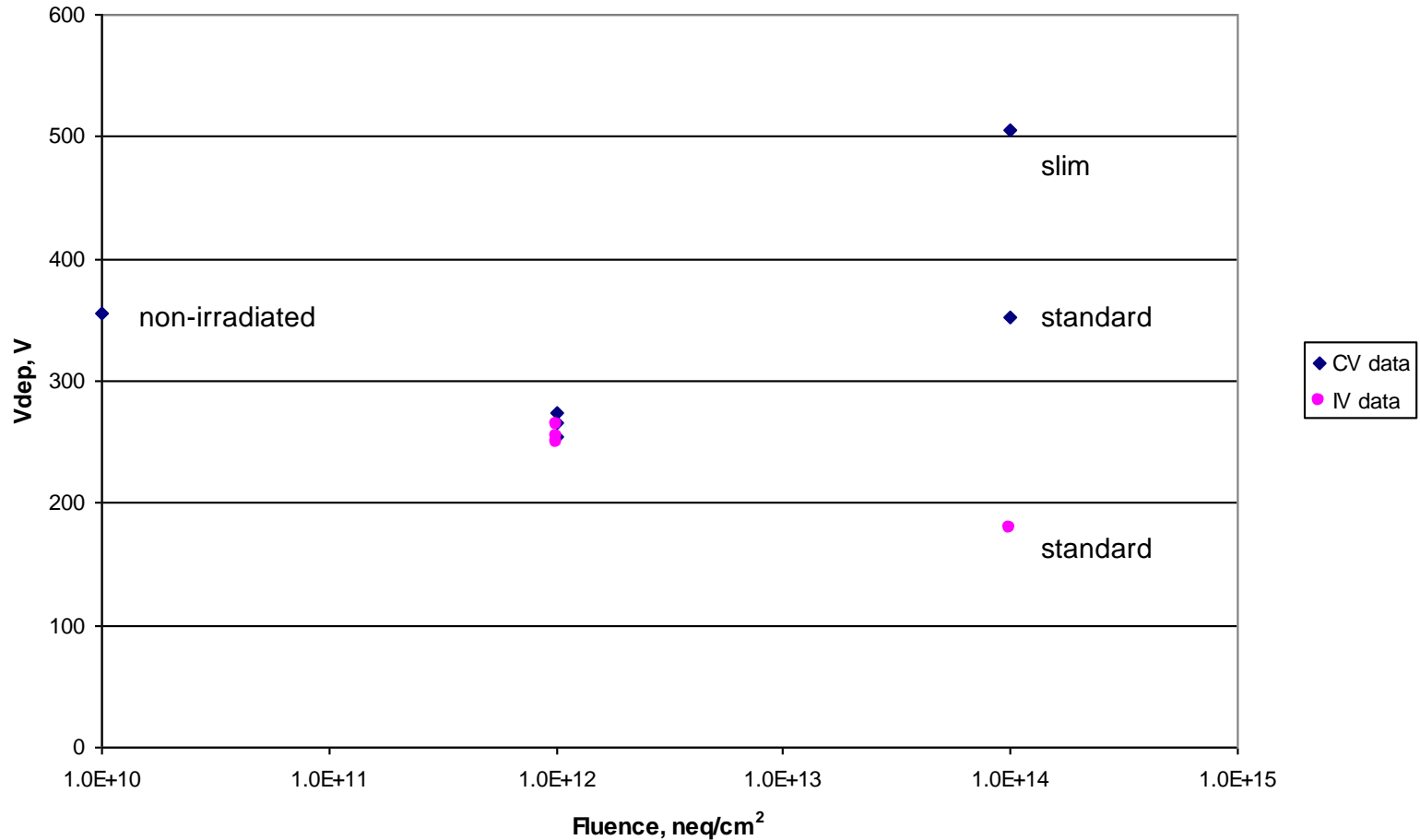
A surprise result: for the sensor irradiated by 10^{14} neq/cm² the CV curves look very strange when the top HT contact is used instead of the back side.

CV for the sensors irradiated by 10^{12} (21C,10kHz) and from 10^{14} to $5 \cdot 10^{15}$ neq/cm² (-25C,400Hz)



CV for all sensors. The line shows the $U^{-0.5}$ dependence. A “kink” exists only up to the 10^{14} neq/cm² fluence. At high bias the curves are distorted by the high current.

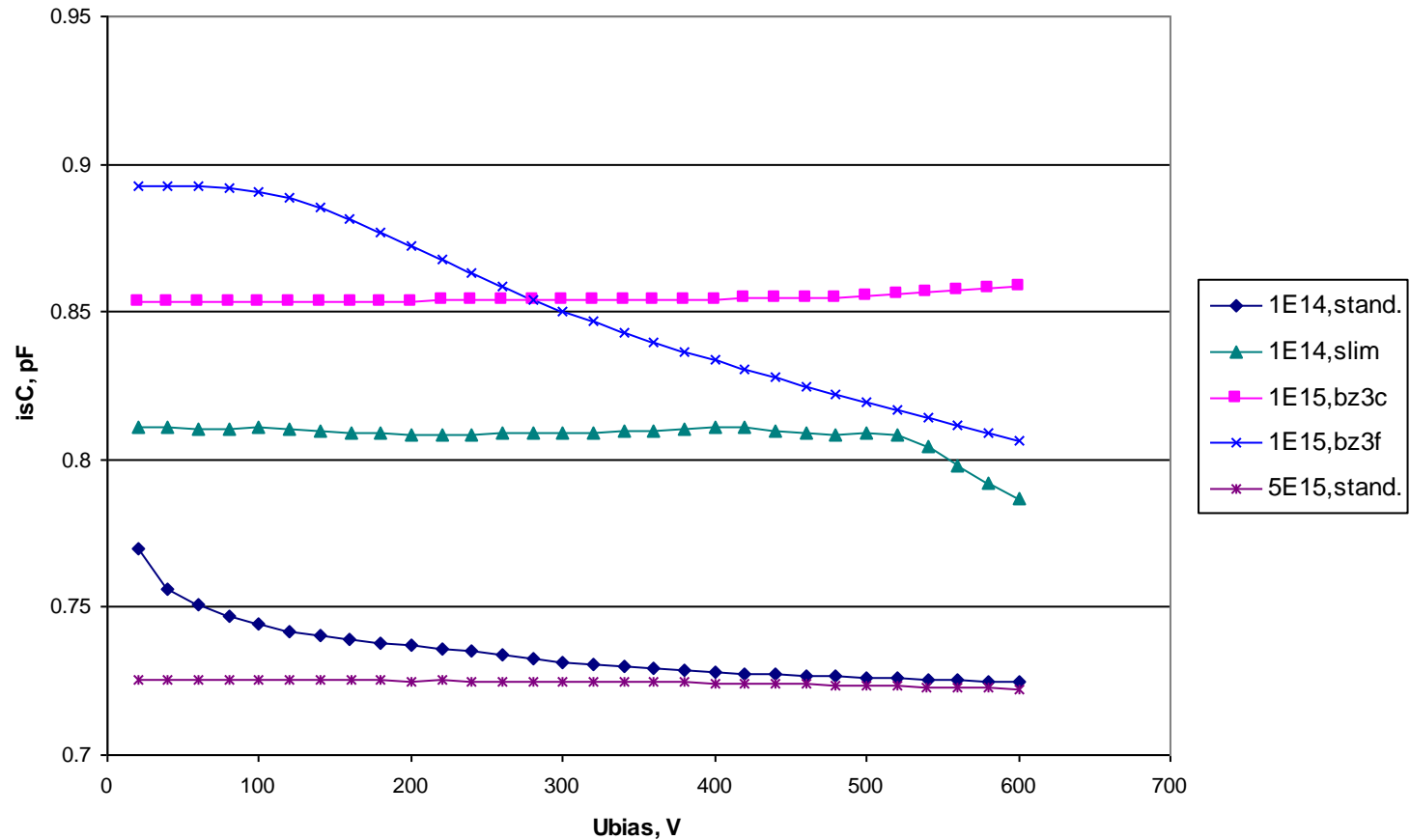
Depletion voltage from CV and IV log-log plots vs fluence



Depletion voltage found from the kink position in the $\log(C)$ vs. $\log(U_b)$ and $\log(I)$ vs. $\log(U_b)$ curves. The value for the non-irradiated sensors is put on the y-axis.

4. Interstrip capacitance

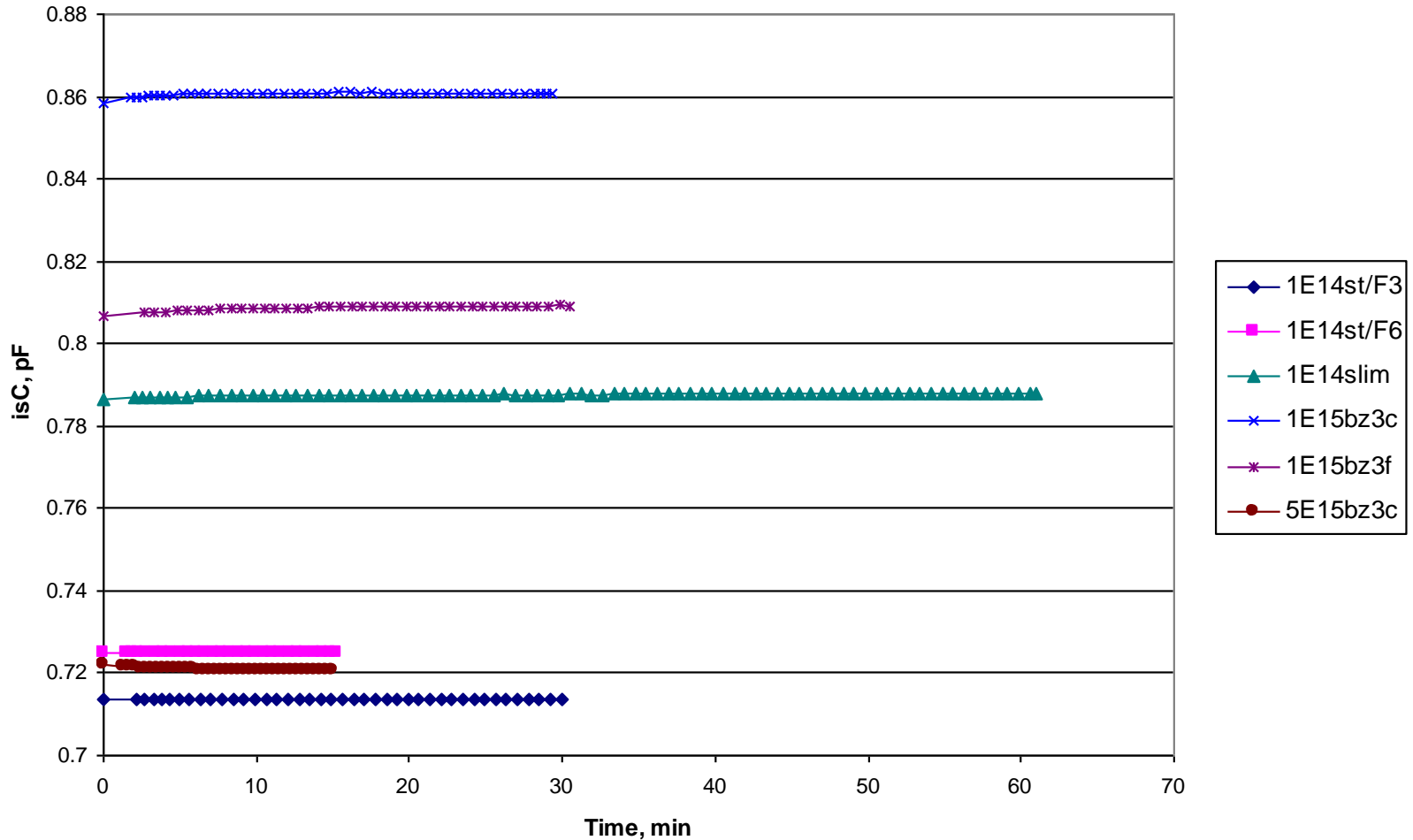
Interstrip capacitance vs bias at -25C for 1 MHz



The capacitance was measured between a strip and its two immediate neighbours. The CV curves here are for 1 MHz frequency.



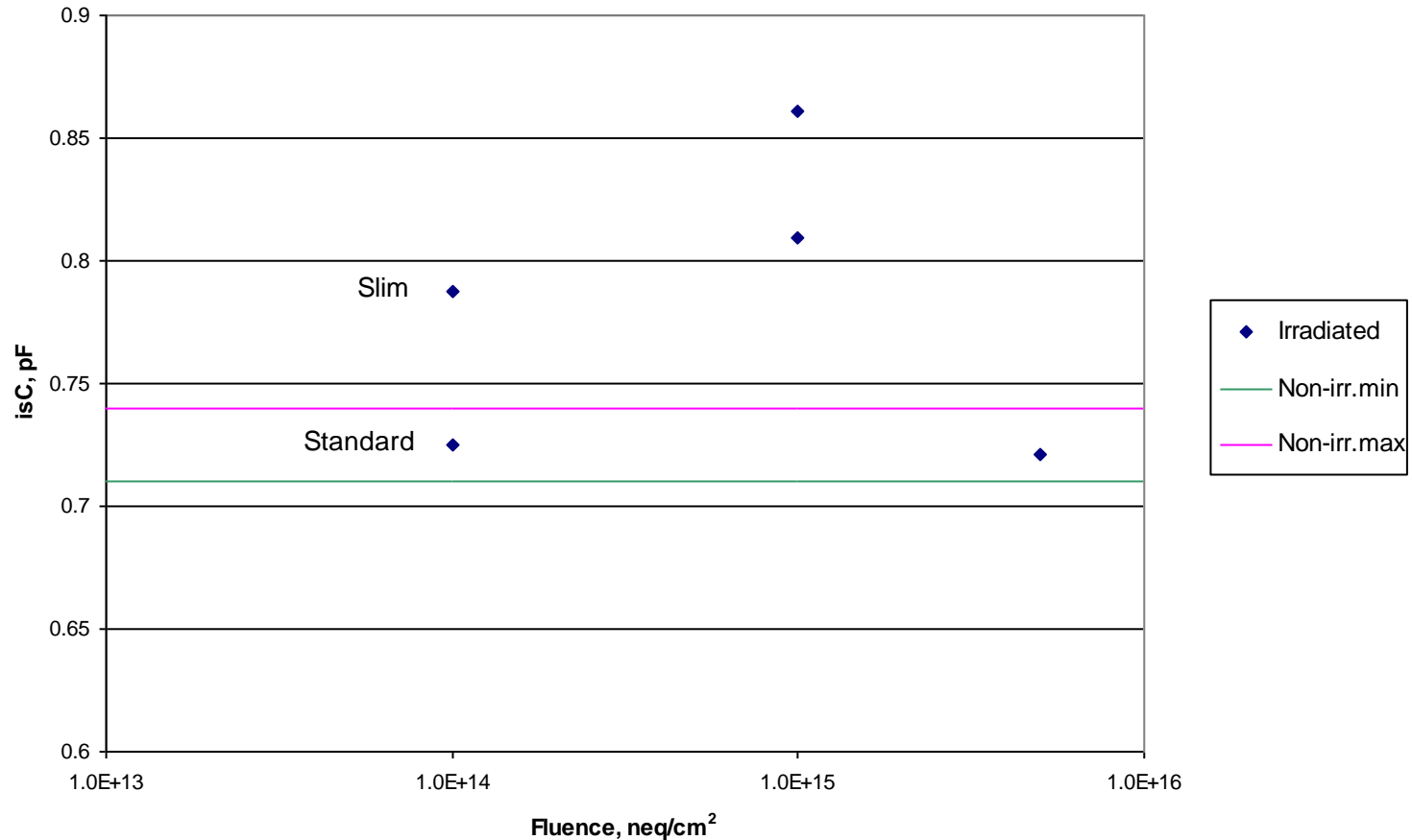
Interstrip capacitance vs time at 600V: temperature -25C, frequency 1MHz



After the bias ramp the capacitance remained stable in time. Standard sensor irradiated by 10^{14} neq/cm² was measured in the test frame 3 with top HT contact and in the frame 6 with the backside contact. The results are close.

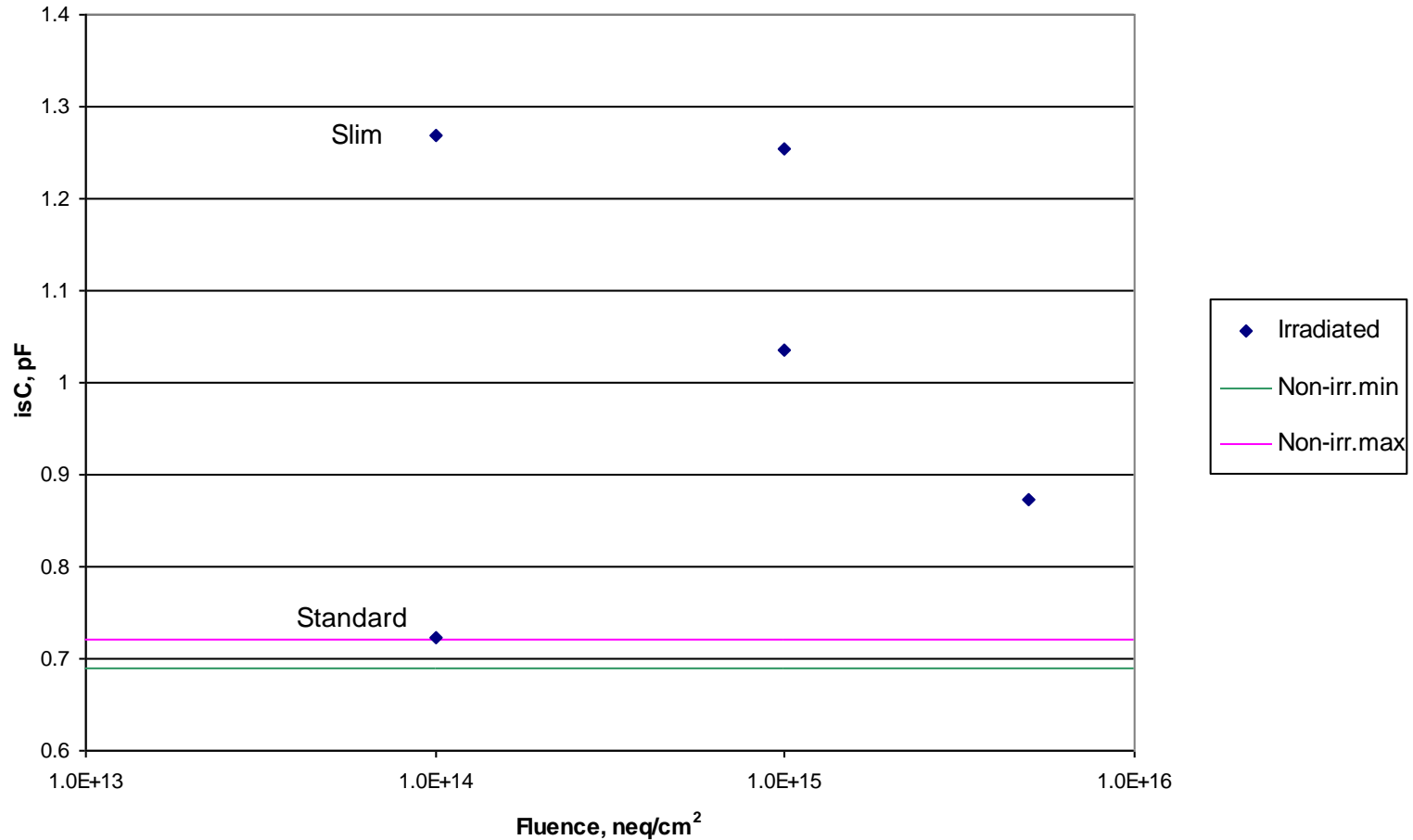


Interstrip capacitance at 600V vs fluence for -25C and 1MHz



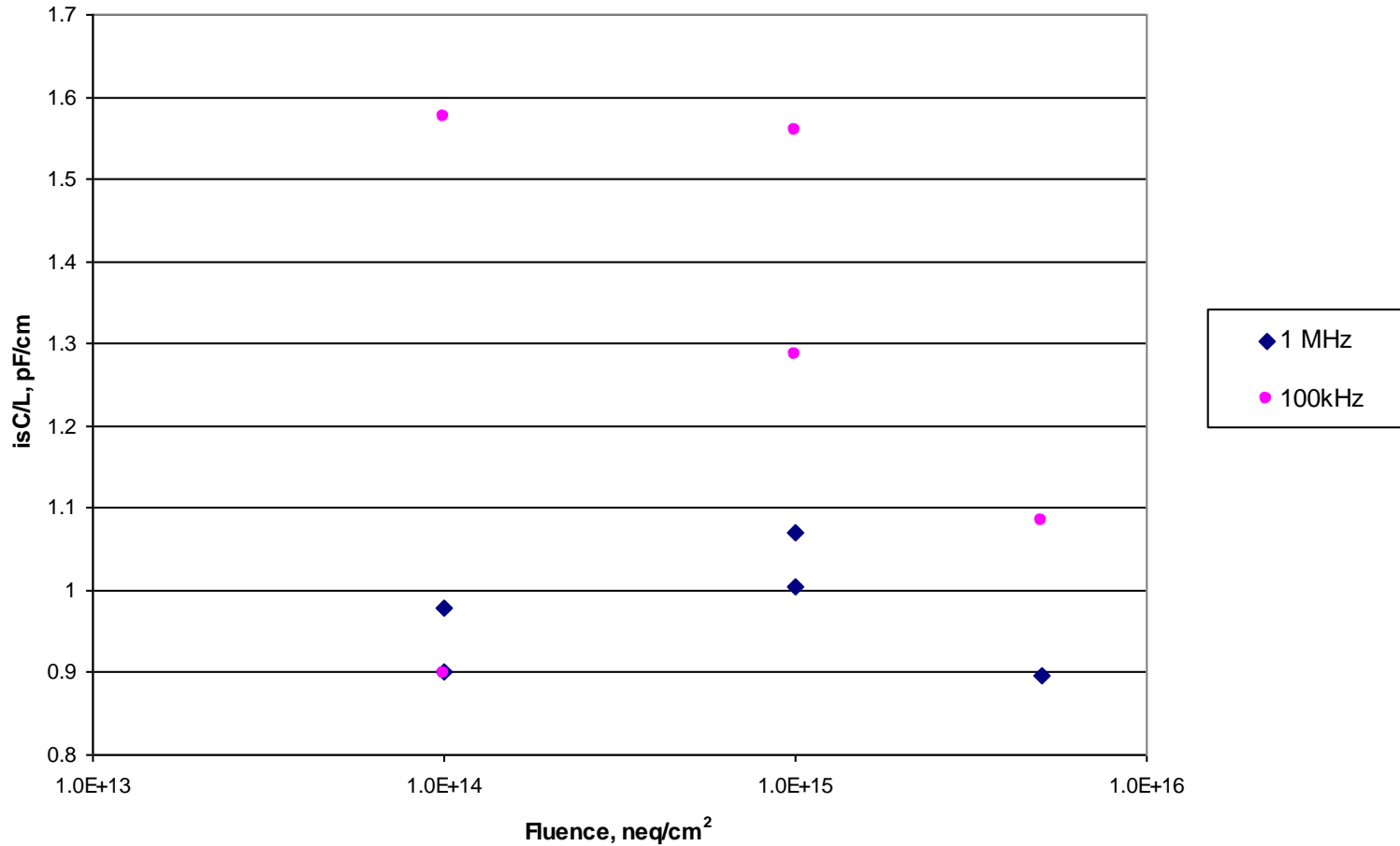
Interstrip capacitance at 1 MHz vs. fluence. The lines show the minimal and maximal values measured in the same conditions with ATLAS 07 un-irradiated sensors. For some irradiated sensors the C_{is} is above the non-irradiation level by up to ~20%.

Interstrip capacitance at 600V vs fluence for -25C and 100 kHz



For 100 kHz the Cis excess in comparison to the non-irradiation level is significantly higher than for 1 MHz.

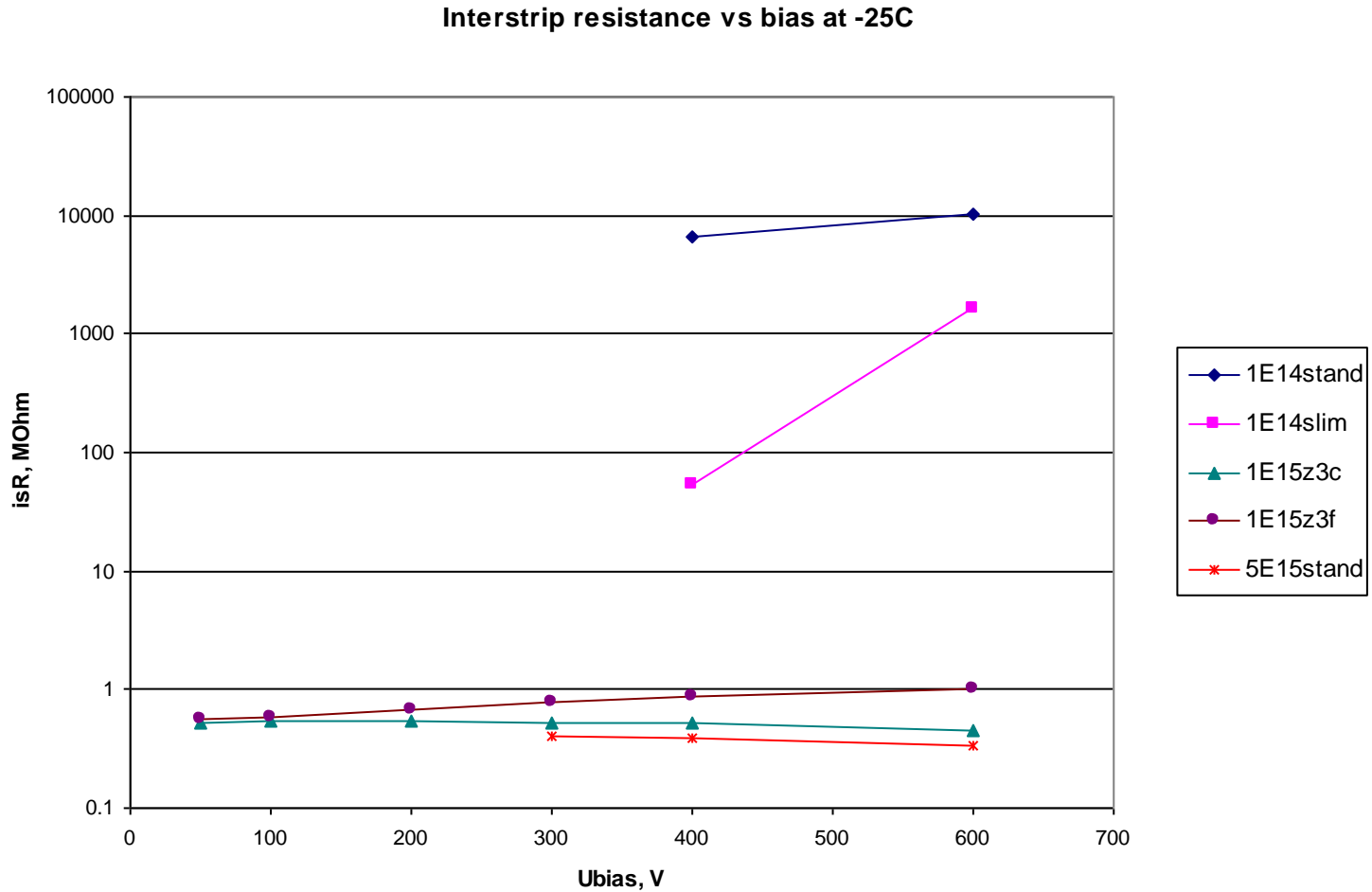
Interstrip capacitance per unit length at 600V vs fluence for 1MHz and 100 kHz at -25C



Normalised by the strip length of 0.80 cm the Cis is noticeably higher than the specs value of 0.8 pF/cm. For more relevant 1 MHz frequency it is closer to the specs.

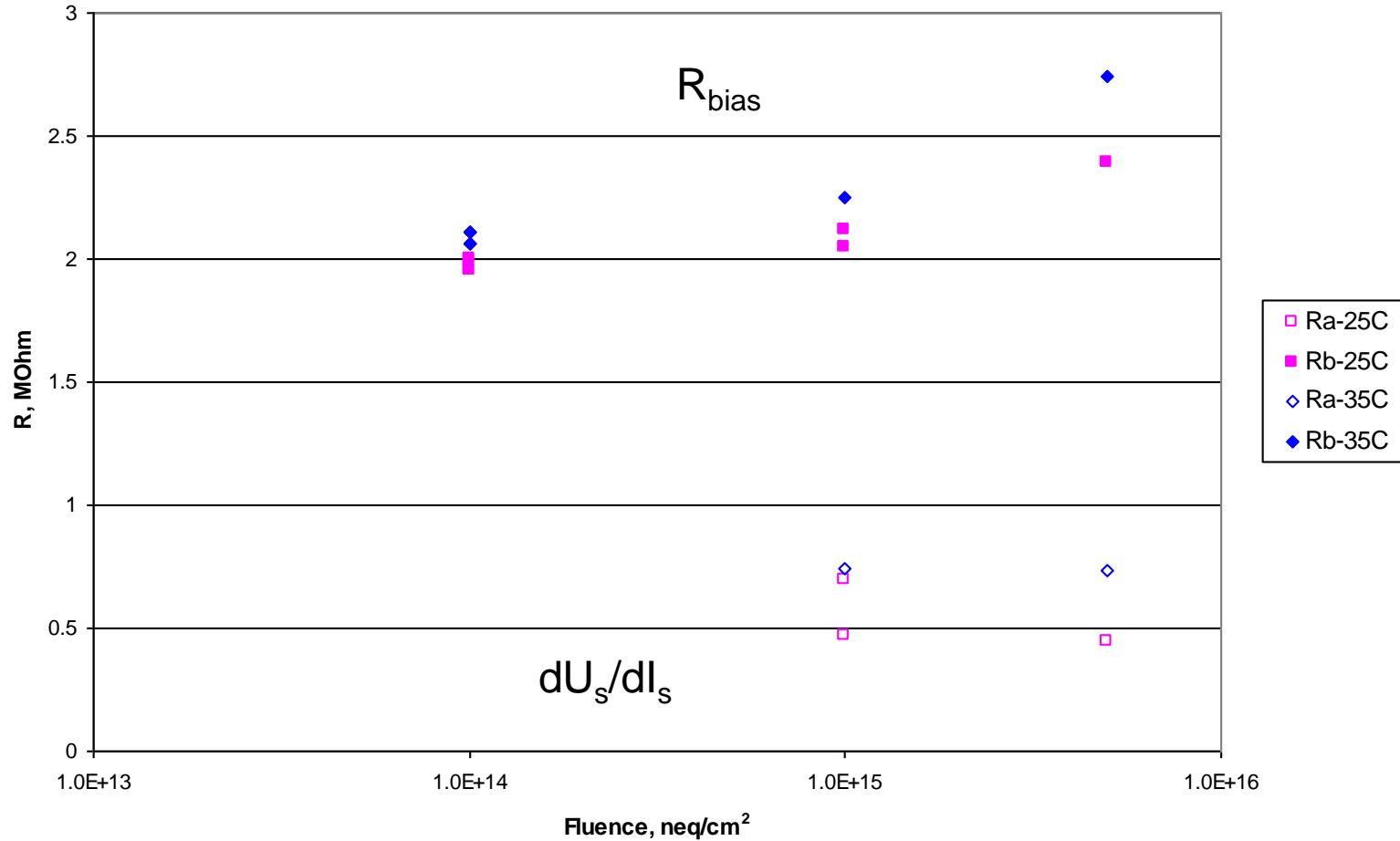


5. Interstrip resistance



For fluences $\geq 10^{15}$ neq/cm² the interstrip resistance drops to 0.3 – 1 MOhm. At -35°C it increases but only by a factor of ~2.

Rbias apparent and reconstructed at -25C and -35C

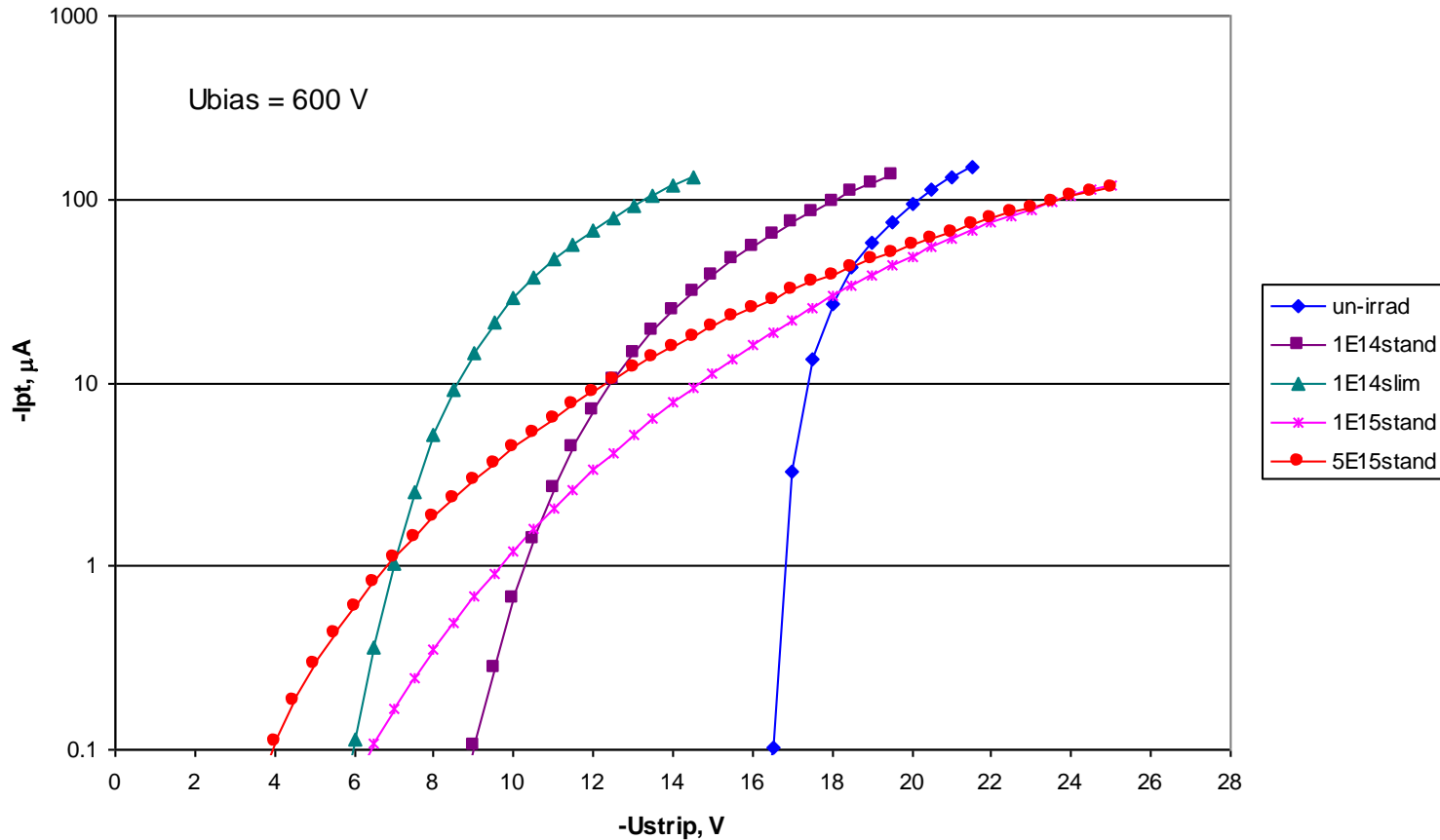


Low interstrip resistance is R makes an apparent bias resistor at the master strip, $R_a = dU_{strip}/dI_{strip}$, much lower than R_{bias} but the reconstructed R_{bias} values are reasonable.



6. Punch-through properties

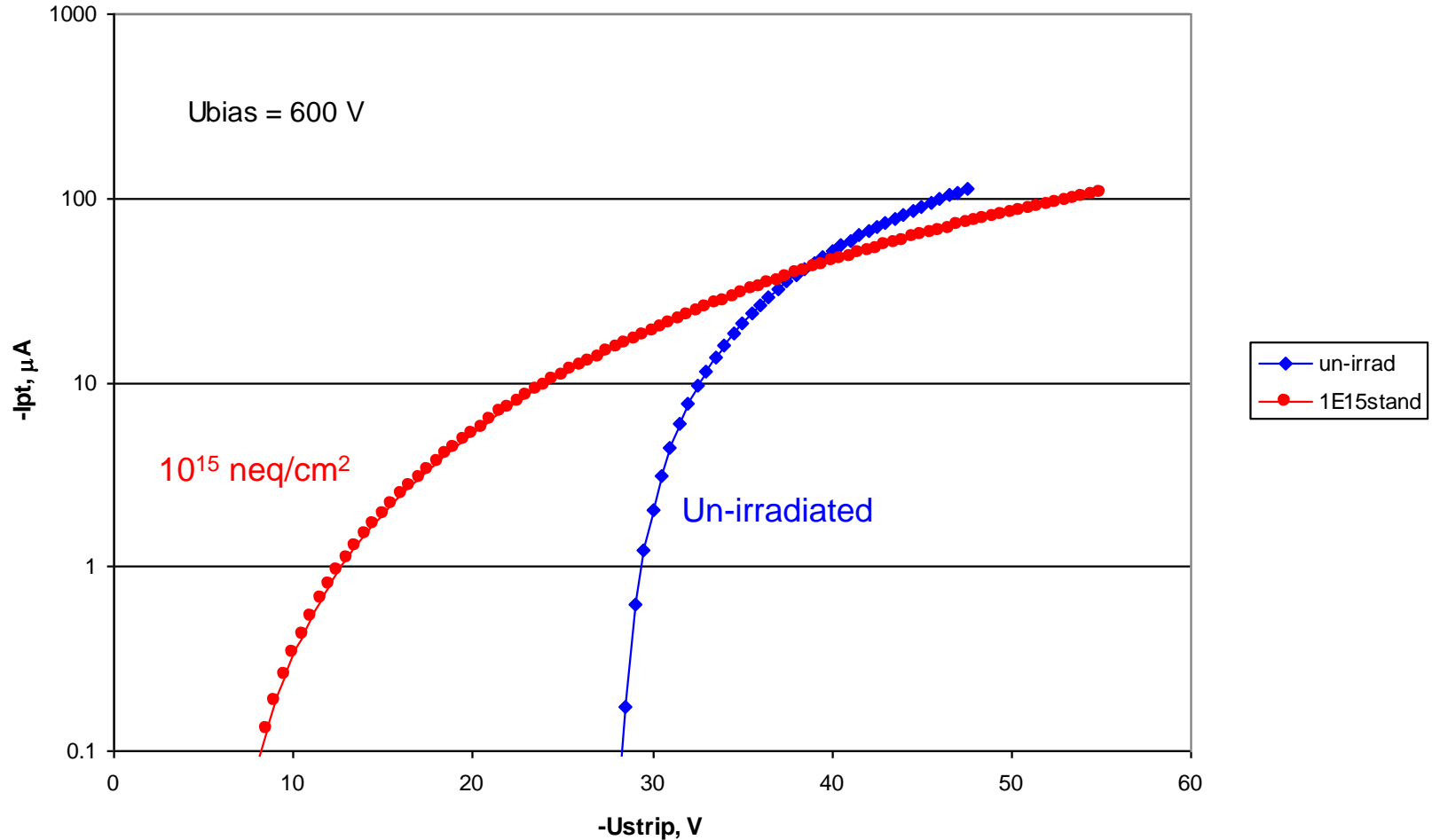
Punch-through current in z3c sensors at -25C (+21C for un-irradiated one)



With irradiation the onset voltage decreases but the PT current gradient becomes less steep. The data here are for the PTP structure z3c implemented in the main sensor.



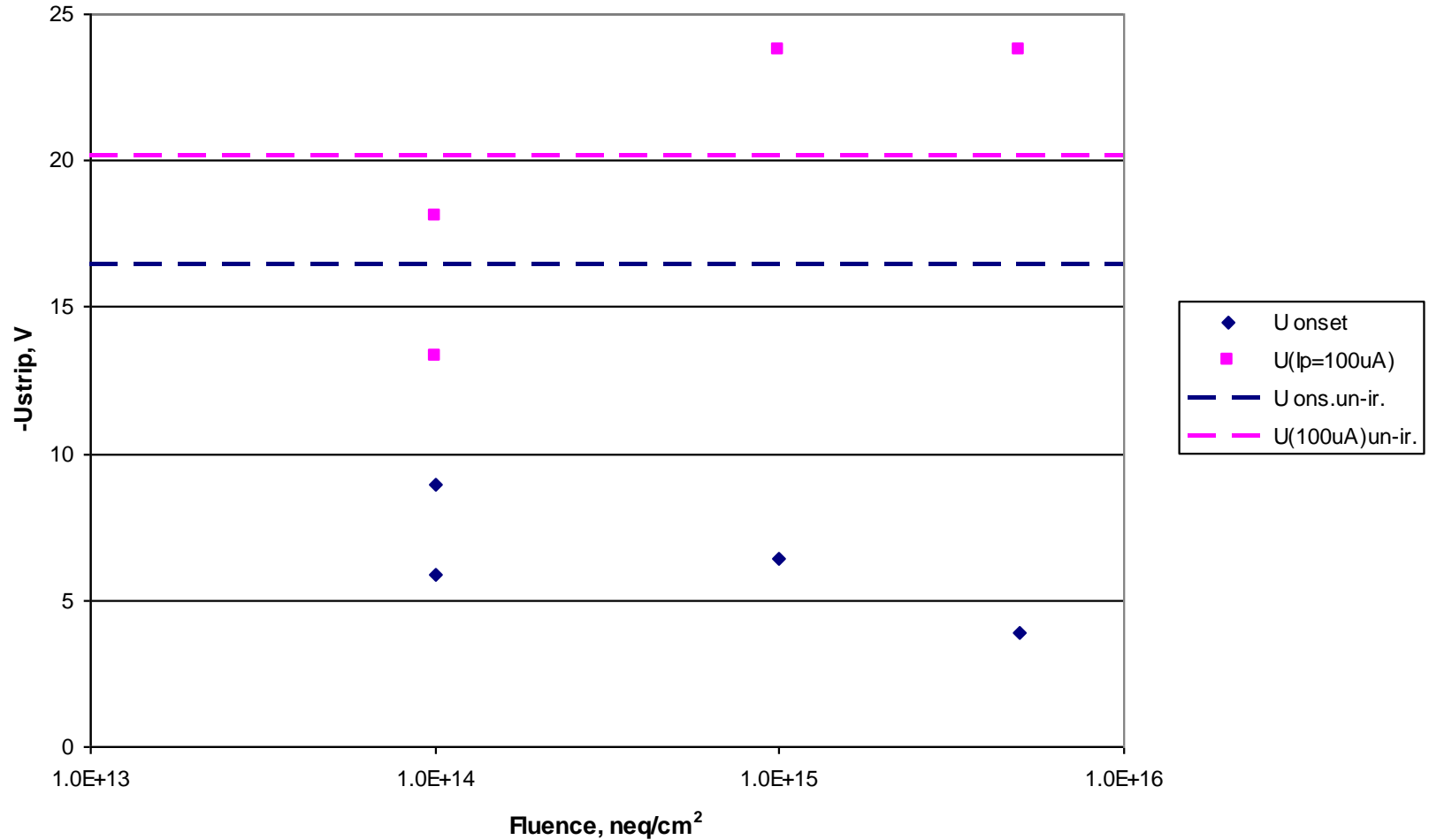
Punch-through current in z3f sensors at -25C (+21C for un-irradiated one)



The same behaviour is observed for the PTP structure z3f though as expected it operates at higher U_{strip} .



Onset voltage and $U(I_{pt}=100\mu A)$ for z3c sensors at 600V and -25C

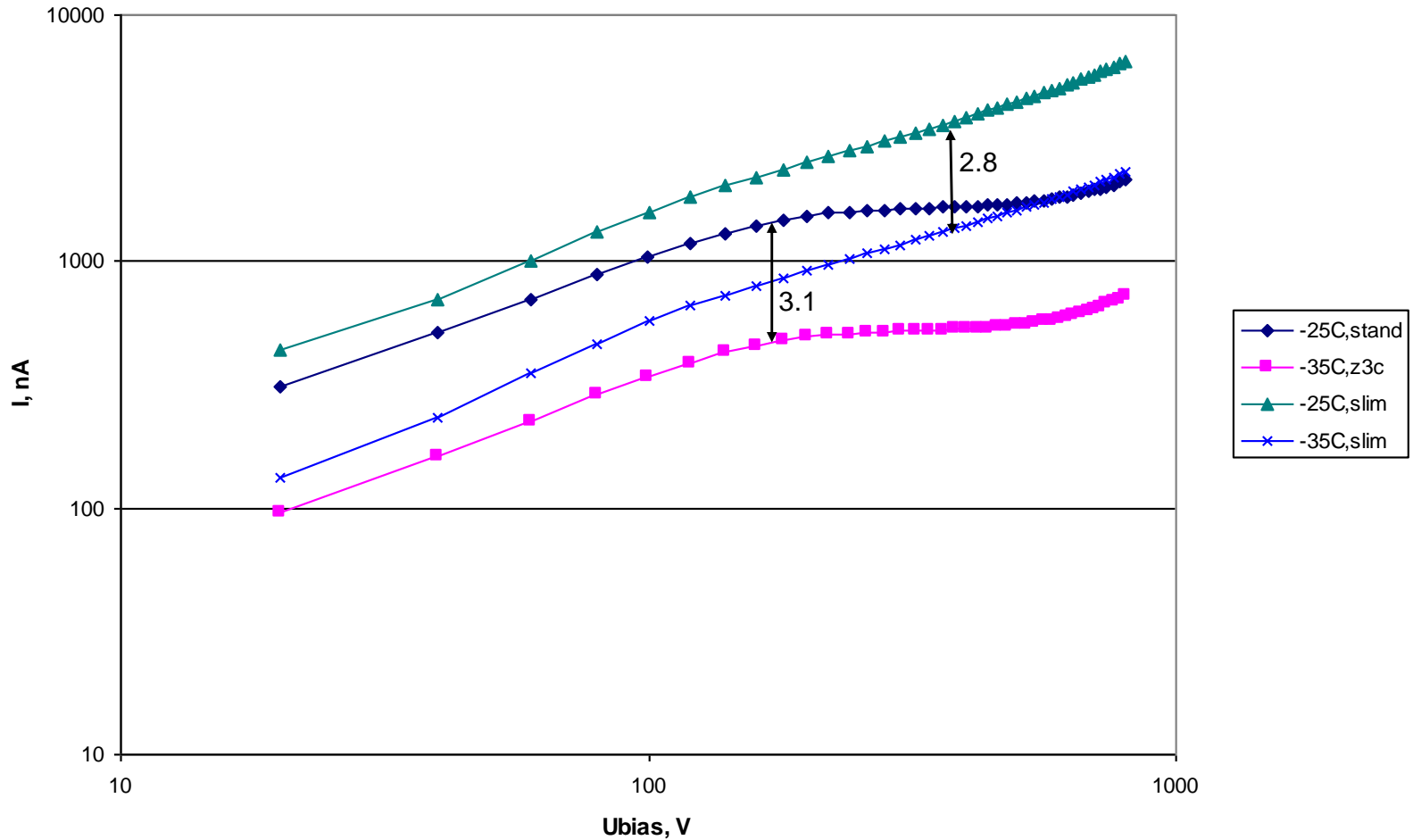


PT onset and the voltage for $I_{pt}=100 \mu A$ in z3c sensors. The lines are the values for the un-irradiated sensor.

7. Conclusions

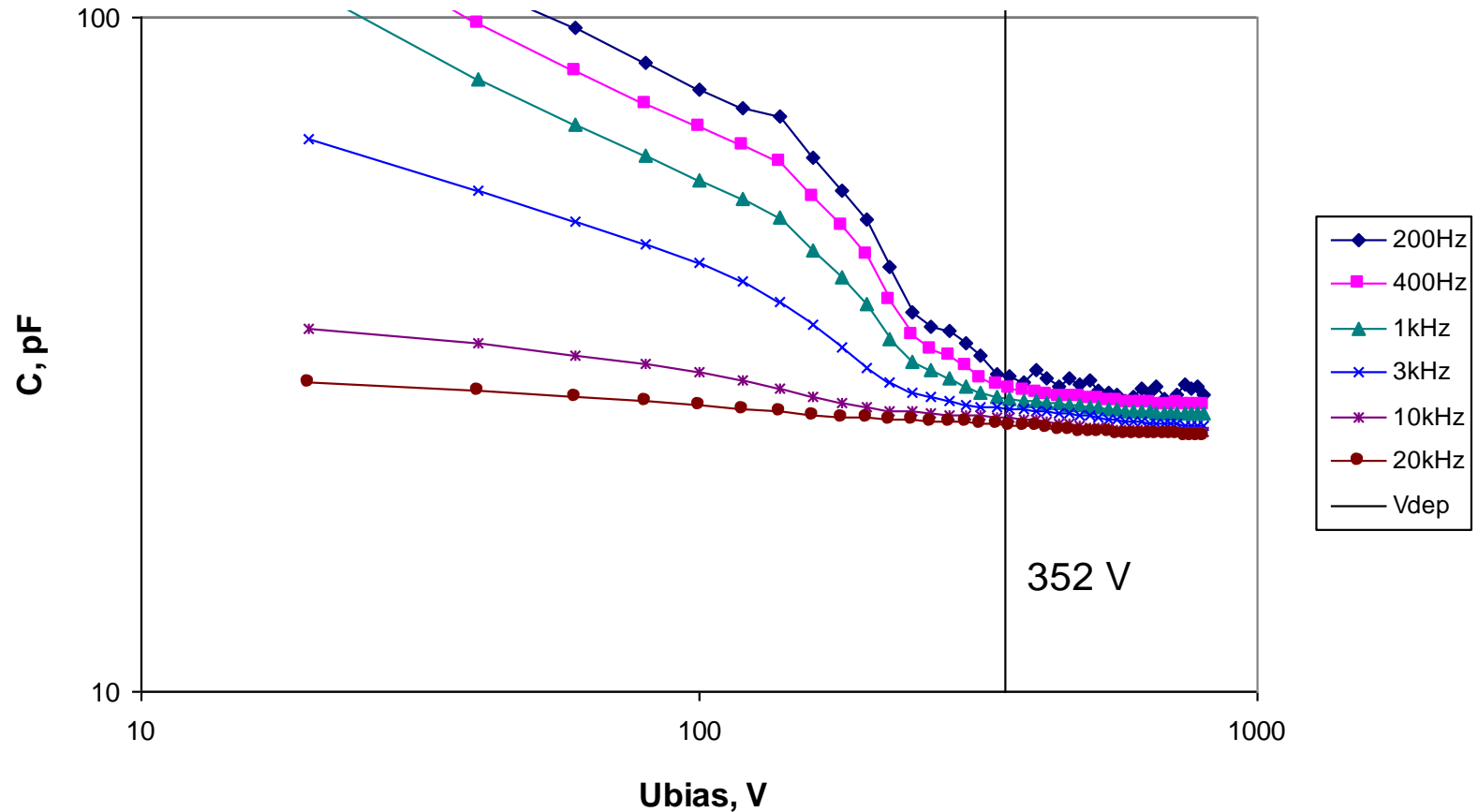
1. The currents in irradiated sensors are higher than anticipated from the pure bulk generation current.
2. Up to the fluence of 10^{14} neq/cm² the depletion voltage remains below 600 V. For higher fluence the CV measurements do not allow V_{dep} measurement.
3. The interstrip capacitance in irradiated sensors may exceed that before irradiation by ~20% at 1 MHz. The excess is even higher at 100 kHz.
4. For the fluence $\geq 10^{15}$ neq/cm² the interstrip resistance drops down to 0.3 -1 M Ω . However it is still large compared to the input impedance of the FE electronics which is of ~1 k Ω .
5. Up to the maximum investigated fluence of $5 \cdot 10^{15}$ neq/cm² the punch-through protection structure of z3c type allows draining of 100 μ A current with the DC voltage at the strip of less than 25 V.
6. The sensors remain fully operational up to the maximum investigated fluence.

Backup slides



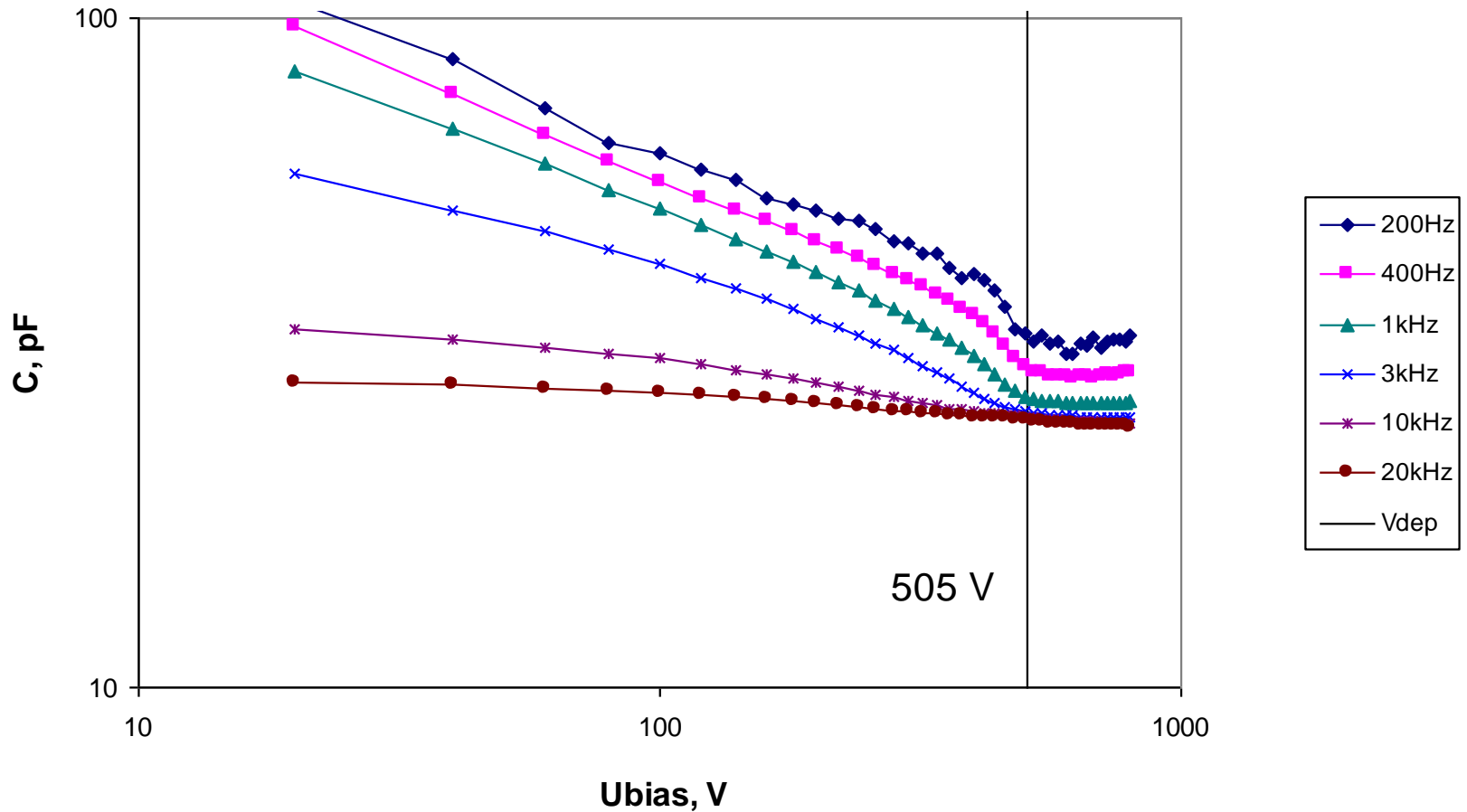
IV at -25°C and -35°C for the standard and slim sensors irradiated by 10^{14} neq.cm². The correction coefficient expected for the bulk generated current is 3.6.

Standard w627-bz3c-p12 irradiated by $1E14$ neq/cm²: CV at -25C and different frequencies



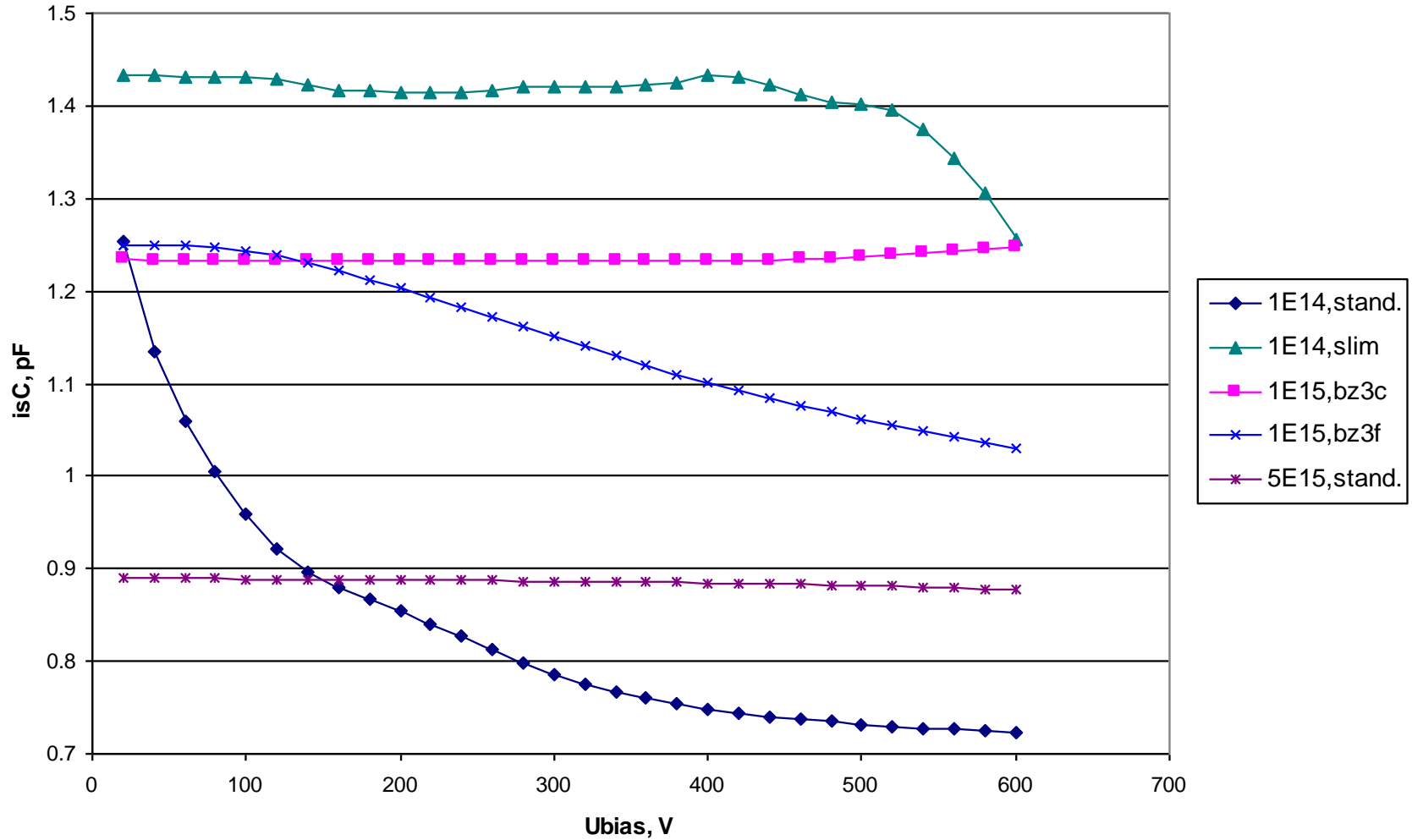
The C_s -V curves at frequencies from 200 Hz to 20 kHz for the standard edge sensor irradiated by 10^{14} neq/cm². The vertical line shows the “kink” position for the 400 Hz curve.

Slim w610-bz3c-p4 irradiated by $1E14$ neq/cm²: CV at -25C and different frequencies

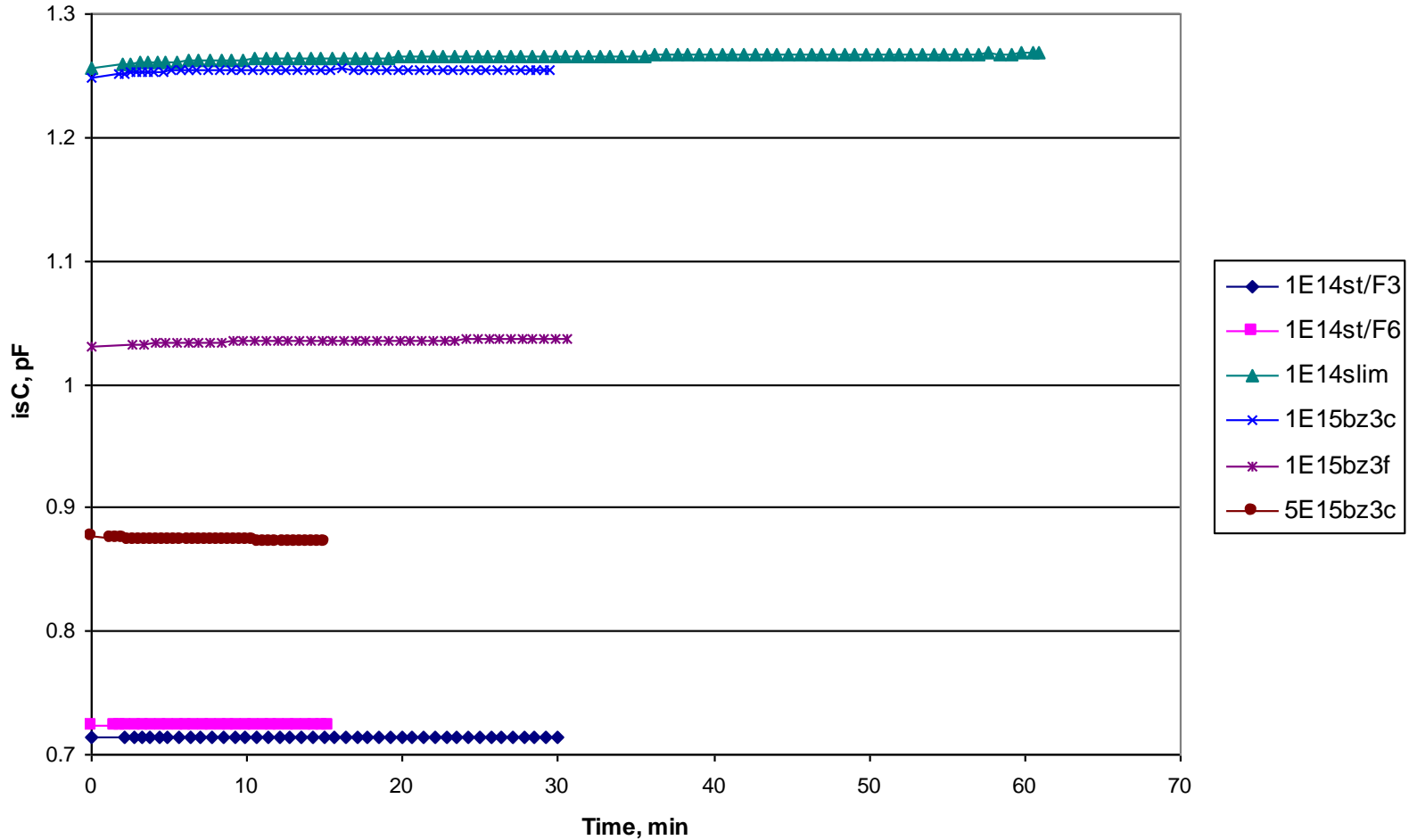


The C_s - V curves at frequencies from 200 Hz to 20 kHz for the slim edge sensor irradiated by 10^{14} neq/cm². The vertical line shows the “kink” position for the 400 Hz curve.

Interstrip capacitance vs bias at -25C for 100 kHz



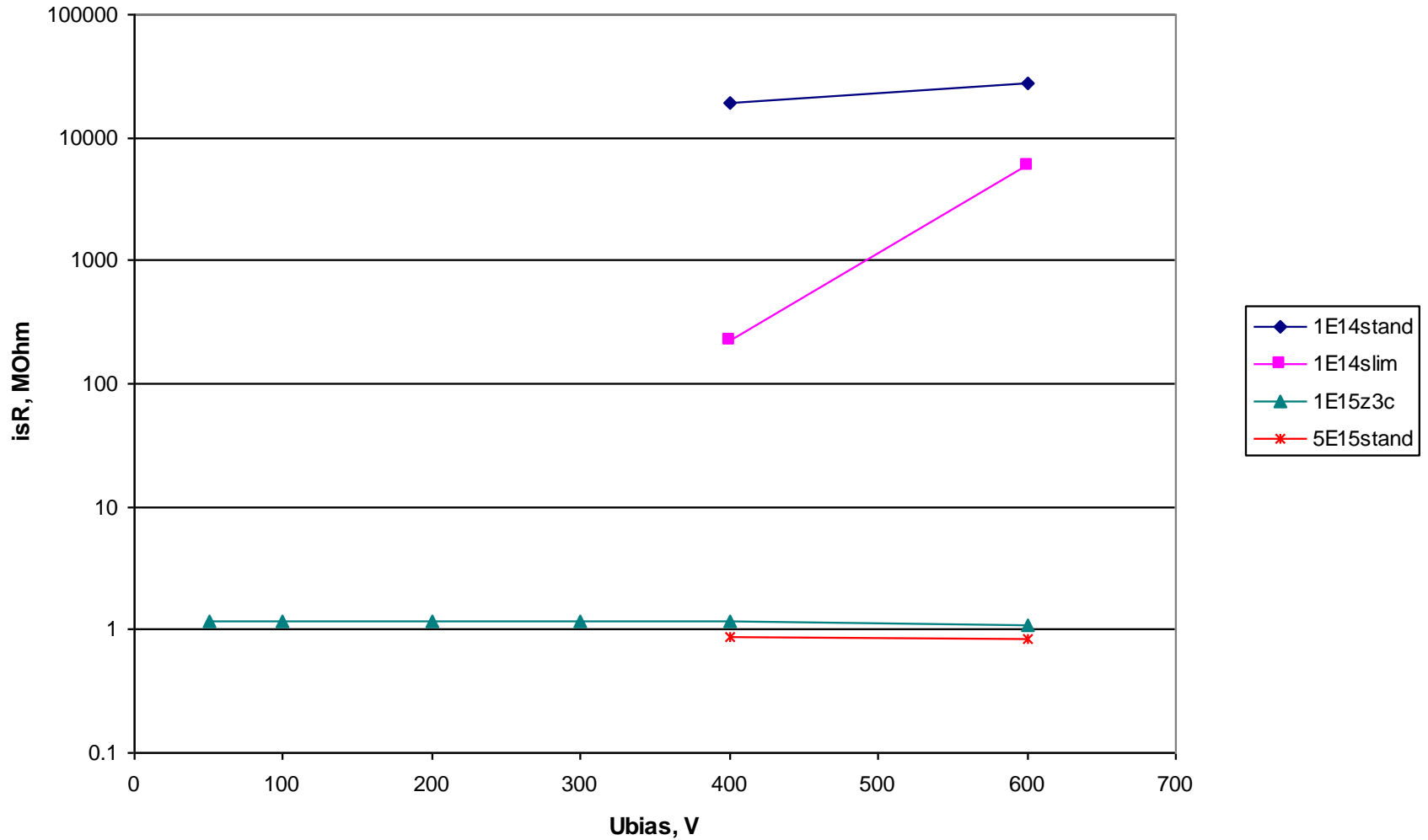
Interstrip capacitance vs time at 600V: temperature -25C, frequency 100 kHz



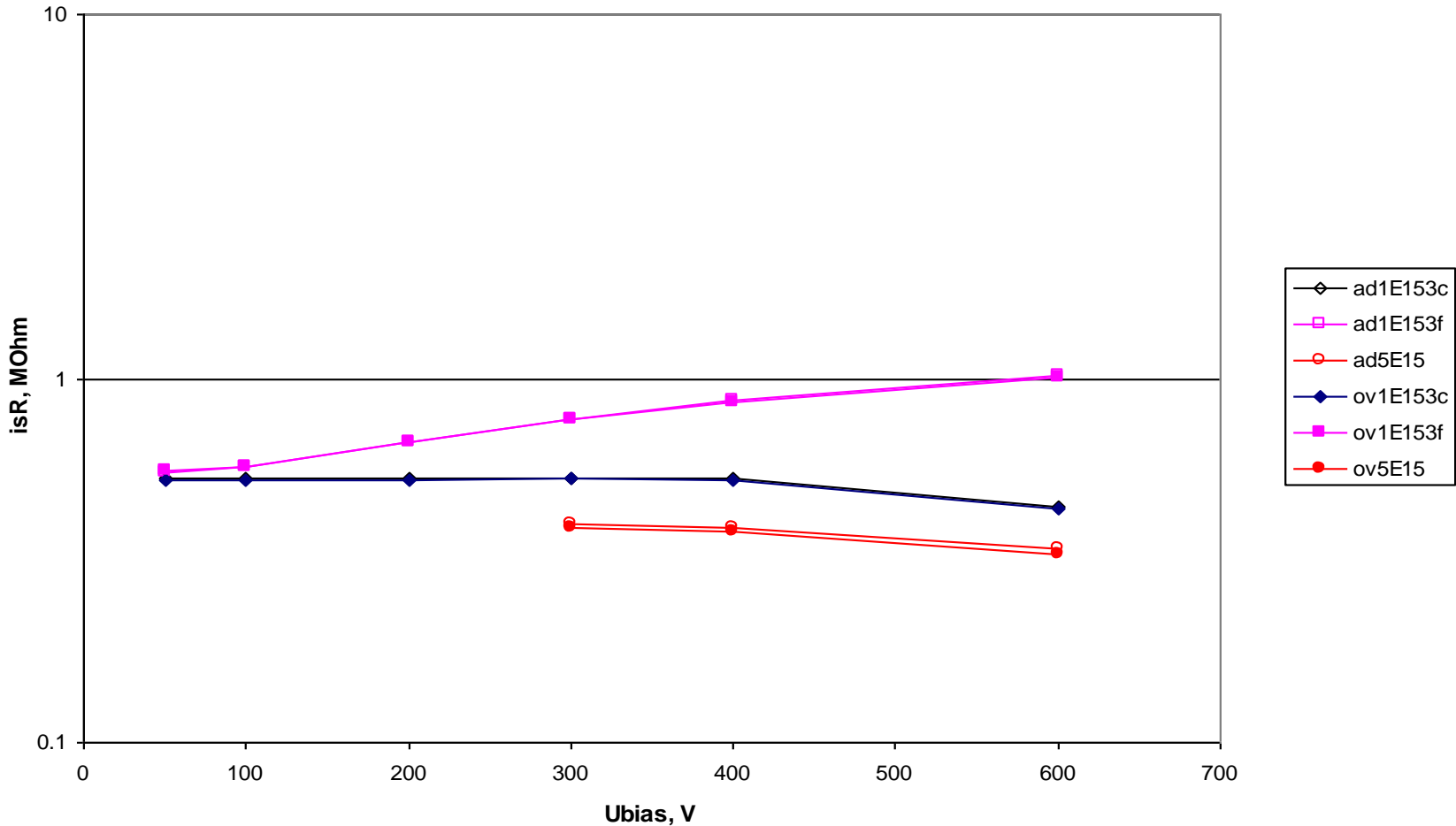
After the bias ramp the capacitance remained stable in time. Standard sensor irradiated by 10^{14} neq/cm² was measured in the test frame 3 with top HT contact and in the frame 6 with the backside contact. The results are close.



Interstrip resistance vs bias at -35C

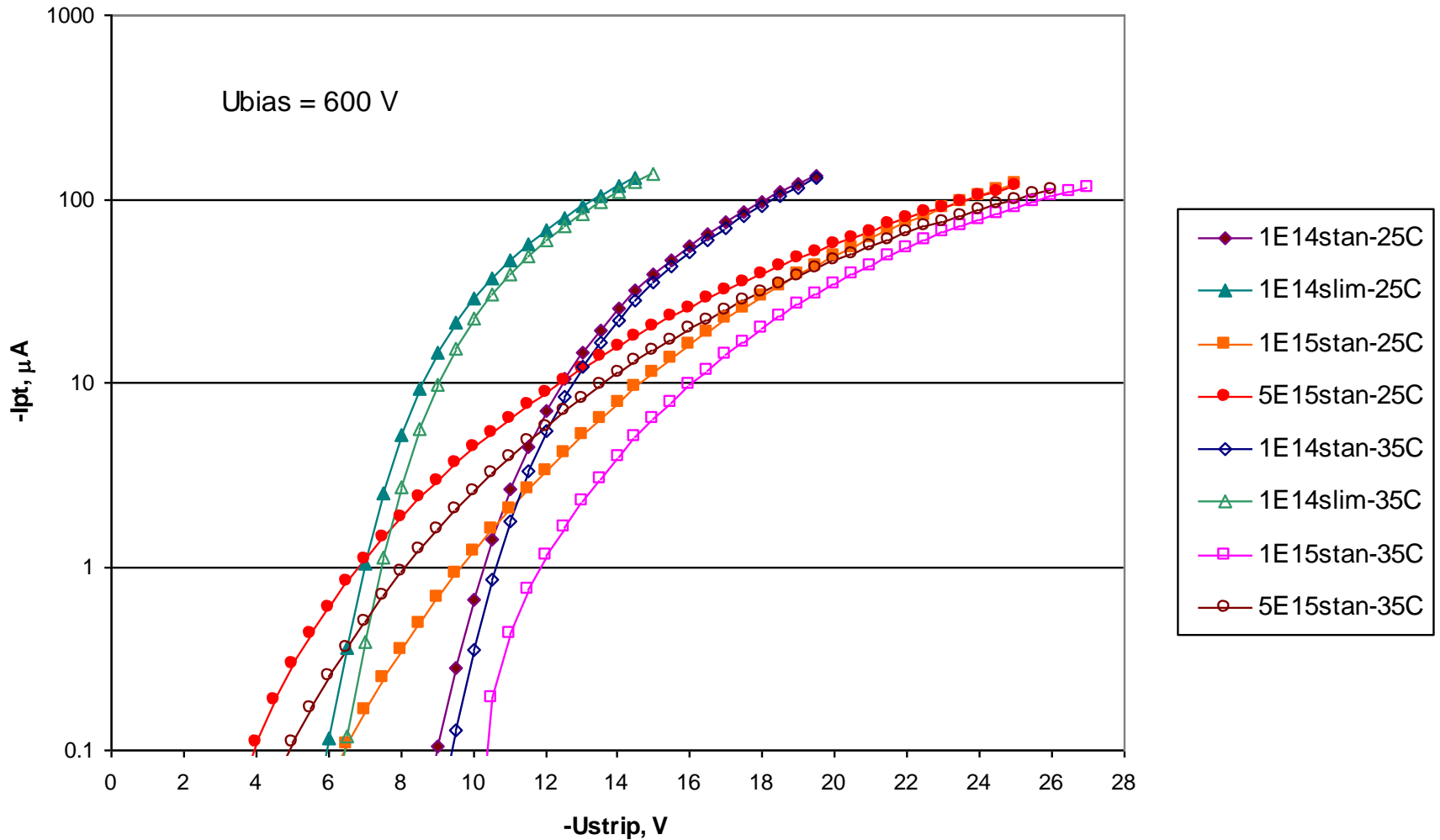


Interstrip resistance vs bias at -25C measured between adjacent strips and over one strip



For low isR it can be measured not only by signal from the adjacent strip but also by that from the next neighbour. The results are close, which confirms the validity of the used simple model with equal isR between all strips.

Punch-through current in z3c sensors at -25C and -35C



The difference between the PT currents at $-25^{\circ}C$ and $-35^{\circ}C$ is small.